

Evaluating Membership Inference Attacks and Defenses in Federated Learning

Gongxi Zhu¹ *, Donghao Li² *, Hanlin Gu³ †,
Yuxing Han⁴, Yuan Yao², Lixin Fan³, Qiang Yang^{2,3}

¹University of Electronic Science and Technology of China,

²The Hong Kong University of Science and Technology,

³Webank, ⁴Tsinghua University

gx.zhu@foxmail.com, dlibf@connect.ust.hk, ghltsl123@gmail.com

Abstract

Membership Inference Attacks (MIAs) pose a growing threat to privacy preservation in federated learning. The semi-honest attacker, e.g., the server, may determine whether a particular sample belongs to a target client according to the observed model information. This paper conducts an evaluation of existing MIAs and corresponding defense strategies. Our evaluation on MIAs reveals two important findings about the trend of MIAs. Firstly, combining model information from multiple communication rounds (Multi-temporal) enhances the overall effectiveness of MIAs compared to utilizing model information from a single epoch. Secondly, incorporating models from non-target clients (Multi-spatial) significantly improves the effectiveness of MIAs, particularly when the clients' data is homogeneous. This highlights the importance of considering the temporal and spatial model information in MIAs. Next, we assess the effectiveness via privacy-utility tradeoff for two type defense mechanisms against MIAs: Gradient Perturbation and Data Replacement. Our results demonstrate that Data Replacement mechanisms achieve a more optimal balance between preserving privacy and maintaining model utility. Therefore, we recommend the adoption of Data Replacement methods as a defense strategy against MIAs. Our code is available in <https://github.com/Liar-Mask/FedMIA>.

1 Introduction

Federated learning (FL) McMahan *et al.* [2016, 2017]; Konečný *et al.* [2016] has emerged as a promising solution for training machine learning models on decentralized data sources while ensuring data privacy. However, the privacy implications of information exchanged during FL have garnered significant research attention. Compare to Gradient Inversion Attacks (GIAs) Zhu *et al.* [2019]; Geiping *et al.* [2020], Membership Inference Attacks (MIAs), which doesn't require the strong assumption as small batch sizes and local

training epochs, are highly overlooked in FL Nasr *et al.* [2019]. MIAs in FL aim to determine whether a specific sample was part of the training dataset of a particular client and are often conducted by adversaries situated at the server side.

This paper firstly seeks to evaluate the risks and further elucidate the trend of Membership Inference Attacks (MIAs) in FL (see overview in Tab. 1). The initial research on MIAs in federated learning (FL) Zari *et al.* [2021] focused on the model of a single communication round and individual clients, utilizing the gradient norm and loss. Subsequently, a series of studies Zhang *et al.* [2020]; Li *et al.* [2022]; Gu *et al.* [2022] leveraged observed model information from multiple communication rounds (Multi-temporal) in FL to enhance the effectiveness of MIAs. In addition to considering the Multi-temporal model information, this paper investigates the impact of utilizing information from multiple clients (Multi-spatial) in the context of MIAs.

Several defense methods have been proposed to mitigate Membership Inference Attacks (MIAs) in federated learning. These defense methods can be categorized into two main categories: gradient perturbation and data replacement. 1) Gradient perturbation methods aims to protect membership by adding perturbation on uploading gradients, including differential privacy Geyer *et al.* [2017]; Zheng *et al.* [2021], gradient quantization Reisizadeh *et al.* [2020]; Haddadpour *et al.* [2021], and gradient sparsification Gupta and Raskar [2018]; Shokri and Shmatikov [2015]; Thapa *et al.* [2022]; 2) Data replacement aims to protect membership by modifying the training data, including Mixup, InstaHide Zhang *et al.* [2017]; Huang *et al.* [2020] and data generation method Lee *et al.* [2021]; Xie *et al.* [2021].

The paper makes two main contributions. Firstly, a comprehensive evaluation is conducted on existing Membership Inference Attack (MIA) techniques in FL Nasr *et al.* [2019]; Li *et al.* [2022]; Zari *et al.* [2021]; Chen *et al.* [2020], as well as the proposed MIA that leverage information from multiple communication rounds and clients' models (see Sect. 3.4). We have two findings in Sect. 4 (see results in Fig. 1): 1) Combining information from multiple epochs improves the overall effectiveness of MIAs compared to using information from a single epoch; 2) Incorporating models from non-target clients significantly enhances the effectiveness of MIAs, particularly when the clients' data is homogeneous. The intuition behind this is that using a non-target model as a shadow model al-

*These authors contributed equally to this work.

†Corresponding author.

Table 1: Overview of MIAs in FL

	Threat Model	Measurement	Temporal Information	Spatial Information
Loss-I Yeom <i>et al.</i> [2018]	Semi-honest Server	Data Loss	Single	Single
Cos-I Li <i>et al.</i> [2022]	Semi-honest Server	Cos Similarity	Single	Single
Grad-Norm Nasr <i>et al.</i> [2019]	Malicious Client	Gradient Norm	Single	Single
Los-II Gu <i>et al.</i> [2022]	Semi-honest Server	Data Loss	Multi	Single
Cos-II Li <i>et al.</i> [2022]	Semi-honest server	Cos Similarity	Single	Single
Grad-Diff Li <i>et al.</i> [2022]	Semi-honest server	Cos similarity	Multi	Single
Loss-III Ours	Semi-honest server	Cos similarity	Multi	Multi
Cos-III Ours	Semi-honest server	Cos similarity	Multi	Multi

lows for confidence estimation of each sample’s membership, thereby identifying samples that are more vulnerable to attacks. Moreover, we investigate the different factors of FL in MIAs (see Sect. 4.3). Secondly, we systemically evaluate two type defense methods (four defenses) via the model performance (utility) and privacy leakage in Sect. 6. Additionally, the utility and privacy leakage trade-offs of these defense methods are further evaluated using hypervolume analysis Zitzler and Künzli [2004]. The experimental results demonstrate that data modifying methods are more effective than gradient perturbation methods in defending against MIAs. Replacing the data helps the model generalize better and avoid overfitting Zhang *et al.* [2017], while still maintaining good model performance. Therefore, it is suggested that modifying data methods be employed to enhance the privacy of Federated Learning against MIAs.

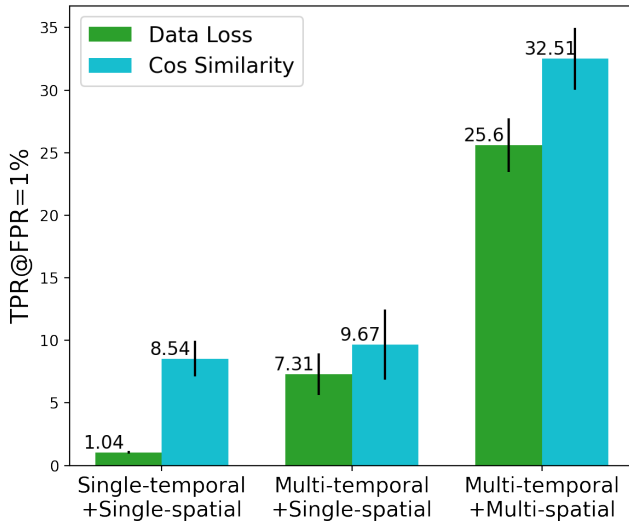


Figure 1: Evaluation of three categories MIAs: MIA I (single-temporal + single-spatial model information), MIA II (multi-temporal + single-spatial model information) and MIA III (multi-temporal + multi-spatial model information). Blue and orange color represent the loss and cos similarity measurement respectively (see details in Sect. 4.1).

2 Related work

2.1 Federated Learning

Federated learning was originally proposed as a collaborative approach for training machine learning models without the need to share private data among multiple parties McMahan *et al.* [2016, 2017]; Konečný *et al.* [2016]; Yang *et al.* [2019]. However, more recently, the concept of “trustworthy federated learning” has been introduced by Kang *et al.* [2023]. This variant of federated learning places a heightened emphasis on the preservation of privacy throughout the federated learning process. This shift in focus reflects the increasing awareness of privacy concerns and the recognition of the importance of robust security measures in federated learning systems

2.2 Membership Inference Attack

MIA is a widely studied privacy attack in centralized learning scenarios. Depending on the information available to the attacker, MIA can be categorized into black-box attack (where only the output predictions of the model can be obtained) [Shokri *et al.*, 2017; Salem *et al.*, 2019; Yeom *et al.*, 2018; Sablayrolles *et al.*, 2019; Song and Mittal, 2020; Choo *et al.*, 2020; Hui *et al.*, 2021; Truex *et al.*, 2019] and white-box attack (where the entire model is available) [Nasr *et al.*, 2019; Rezaei and Liu, 2020].

In the context of federated learning, Nasr *et al.* Nasr *et al.* [2019] first analyzed membership inference attacks in federated learning and proposed both passive and active attacks. In a passive attack, the attacker solely focuses on obtaining membership leaks based on accessible information without disrupting or compromising the normal training process. Conversely, an active attack involves the ability to modify the updates of federated learning, thereby increasing the vulnerability of the trained models to attacks. Zari *et al.* Zari *et al.* [2021] proposed a membership inference attack for federated learning that utilizes the probabilities of correct labels under local models at different epochs for inference. However, this approach requires member samples for auxiliary attacks. Li *et al.* Li *et al.* [2022] proposed a passive membership inference attack that does not require training on member samples. They designed two metric features based on the orthogonality of gradients to distinguish whether a sample is a member.

3 Membership Inference Attacks in FL

3.1 Setting

We consider a *horizontal federated learning* (HFL) Yang *et al.* [2019]; McMahan *et al.* [2017] setting consisting of one server and K clients. We assume K clients have their local dataset $D_k = \{(x_{k,i}, y_{k,i})\}_{i=1}^{n_k}, k = 1 \cdots K$, where $x_{k,i}$ is the input data, $y_{k,i}$ is the label and n_k is the total number of data points for k_{th} client. Since we focus on evaluating membership on each client, we further assume D_k are disjoint. K clients collaboratively train a HFL model w (F_w) to optimize the following objective:

$$\min_w \sum_{k=1}^K \sum_{i=1}^{n_k} \frac{\ell(F_w(x_{k,i}), y_{k,i})}{n_1 + \cdots + n_K}, \quad (1)$$

where ℓ is the loss, e.g., the cross-entropy loss. This paper considers a **semi-honest** attacker (i.e., the server), who desires to determine whether a specific sample (x, y) belongs to k_{th} client's dataset D_k based on the observed model updates for each communication round.

3.2 Trend of MIAs in FL

This section illustrates the trend of MIAs by leveraging the different model information. **MIAs via Single-Temporal and Single-Spatial Information** Nasr *et al.* [2019]; Yeom *et al.* [2018] focused on predicting membership in federated learning based on specific model weights w_k^t , where w_k^t represents the model weights of client k at the t_{th} communication round. The adversaries aim to perform the attack \mathcal{A} as a binary classification task, defined as follows:

$$\mathcal{A}(x, y, w_k^t) = \begin{cases} 1, & \text{if } (x, y) \in D_k \\ 0, & \text{otherwise} \end{cases} \quad (2)$$

Remark. *It is important to note that the adversaries have access to the model, making the membership inference attacks in federated learning a white-box setting.*

MIAs via Single-Temporal and Single-Spatial Information Gu *et al.* [2022]; Li *et al.* [2022] improved upon previous attacks by leveraging multiple pieces of information from communication rounds. As the attackers can continuously observe the model during federated training, they can utilize the changes in loss or gradients of the target data to infer membership information. Specifically, the attackers implement the attack \mathcal{A} based on a series of federated models $\{w_k^t\}_{t=1}^T$ as follows:

$$\mathcal{A}(x, y, \{w_k^t\}_{t=1}^T) = \begin{cases} 1, & \text{if } (x, y) \in D_k \\ 0, & \text{otherwise} \end{cases} \quad (3)$$

MIAs via Multi-Temporal and Multi-Spatial Information (see the proposed method in Sect. 3.4) enhanced MIAs by leveraging the information from non-target models, which are models of non-target clients. The idea behind this is that non-target models can be treated as shadow models that mimic the behavior of the target model. By using multiple shadow models, it becomes possible to accurately infer the membership of target data. One approach is to build an attack model based on the labeled inputs and outputs of the shadow models, and

then use this attack model to estimate membership Shokri *et al.* [2017].

Specifically, the attackers implement the attack \mathcal{A} based on a series of federated models $\mathcal{W} = \{w_k^t | t \in [T], k \in [K]\}$ as follows:

$$\mathcal{A}(x, y, \mathcal{W}) = \begin{cases} 1, & \text{if } (x, y) \in D_k \\ 0, & \text{otherwise} \end{cases} \quad (4)$$

Remark. *It is worth noting that when the clients' data follows a homogeneous distribution, the non-target model is similar to the target model, allowing for accurate membership estimation. However, when the clients' data distribution becomes heterogeneous, the accuracy of membership estimation for non-target models may be affected, which can impact the effectiveness of MIAs (as shown in the results in Section 4.3).*

3.3 The Measurement of MIAs in FL

There are three types of measurement $M(\cdot)$ of MIAs in FL:

- Measurement $M(\cdot)$ is the data **loss** Yeom *et al.* [2018], i.e.,

$$M(x, y, w) = \ell(x, y, w). \quad (5)$$

When the model trained the target data, the loss becomes small.

- Measurement $M(\cdot)$ is the **gradient norm** Nasr *et al.* [2019], i.e.,

$$M(x, y, w) = \left\| \frac{\partial \ell(w, x, y)}{\partial w} \right\|. \quad (6)$$

When the model trained the target data, the gradient norm of the target data becomes small.

- Measurement $M(\cdot)$ is the **cosine similarity** of sample gradient and local update (∇F) Li *et al.* [2022], i.e.,

$$M(x, y, w) = \frac{\langle \nabla F, \frac{\partial \ell(w, x, y)}{\partial w} \rangle}{\|\nabla F\| \left\| \frac{\partial \ell(w, x, y)}{\partial w} \right\|}, \quad (7)$$

where ∇F is uploaded gradients of the target client. According to Li *et al.* [2023], the gradients of different samples in an overparameterized model are orthogonal. Therefore, if (x, y) do not contribute to ∇F , the cosine similarity should be zero and a high cosine similarity indicates the presence of a member in the local updates.

3.4 The proposed MIAs Utilizing Multi-Temporal and Spatial Information

We aim to develop an MIA framework that maximizes information utilization from clients and communication rounds. To achieve this, we propose a three-step MIA framework, addressing the limited utilization of information in previous works Yeom *et al.* [2018]; Nasr *et al.* [2019]; Li *et al.* [2022].

Step 1: Calculating Membership Disclosure Measure based on single target model and epoch

We compute the Membership Disclosure Measure relying on the term cosine similarity Li *et al.* [2022] as Eq. (7) or data loss Yeom *et al.* [2018] as Eq. (5) to denote $M(x, y, w)$ for sample (x, y) on the k -th client.

Step 2: Constructing per-sample hypothesis test using MDM from non-target clients.

Performing hypothesis testing for each individual sample enables estimation of the confidence of the decision. Thus facilitating the selection of high-confidence samples to enhance attack effectiveness Carlini *et al.* [2022]. The following presents the hypothesis test constructed for the sample (x, y) .

$$H_0 : (x, y) \notin D_i \quad H_1 : (x, y) \in D_i \quad (8)$$

As we use MDM to predict membership, we have:

$$H_0 : M(x, y, i) \sim Q \quad H_1 : \text{Otherwise} \quad (9)$$

Where Q is the distribution of M with models trained without sample (x, y) . To estimate Q , previous methods assumed training numerous shadow models, such as Carlini *et al.* [2022], with data that has the same distribution as the training data.

Moreover, we observed that in each local client, $w_k, k \in [K]$ is updated exclusively using data from D_k . Therefore, for $j \neq k$, local models from the j -th client can be treated as shadow models for the k -th client. This observation enables us a practical and resource-efficient approach to estimate Q and calculate the Type-I error rate, specifically, when assuming $Q \sim N(\mu_k, \sigma_k^2)$, where $\mu_k = \frac{1}{K-1} \sum_{j \neq k} M(x, y, w_j)$, $\sigma_k^2 = \frac{1}{K-1} \sum_{j \neq k} (M(x, y, w_j) - \mu_k)^2$, the Type-I error rate can be calculated by:

$$Pr(M(x, y, w_k) > \mu_k) = 1 - \int_{-\infty}^{M(x, y, w_k)} \frac{1}{\sqrt{2\pi\sigma_k^2}} e^{-\frac{(x-\mu_k)^2}{2\sigma_k^2}} dx \quad (10)$$

Step 3: Aggregating p-values from multiple communication rounds.

In the previous step, we demonstrated the estimation of Type-I error rate from a single round. Based on multiple testing theory, we estimate the probability of at least one test being wrong, which can be seen as family-wise error rate Toothaker [1993]:

$$Pr\left(\bigcup_{t=1}^T A_j\right) \leq \sum_{t=1}^T Pr(M(x, y, w_k^t) > \mu_k) \quad (11)$$

where event A_j represents the incorrect rejection of the null hypothesis in the j -th round, \bigcup denotes the union operation and we use Boole’s inequality to give an estimation of its upper bound.

Formulation of the Proposed Method

The proposed MIA method $\mathcal{A}(x, y, \mathcal{W}, k)$ utilizing the multi-temporal and multi-spatial information can be formulated as:

$$\mathcal{A}(x, y, \mathcal{W}) = \mathbb{I}_{\sum_{t=1}^T Pr(M(x, y, w_k^t, k) > \mu_k)}, \quad (12)$$

where \mathbb{I} is indicator function and μ_k and $\mathcal{W} = \{w_k^t | t \in [T], k \in [K]\}$.

4 Evaluation of MIAs in FL

4.1 Experimental Setup

Dataset. In the experiment, we utilized two image classification datasets: CIFAR-100 Krizhevsky *et al.* and Dermnet

Aboulmira *et al.* [2022]. CIFAR-100 contains 50,000 images and 100 categories. Dermnet includes 23,000 dermoscopic images with 23 categories. If there are no additional instructions, each experiment has 10 clients, 300 synchronous communication rounds, and is repeated more than 3 times. For more experimental details, please see Appendix A.1.

MIAs. We conducted a comprehensive comparison of various baseline attack methods and we classified existing methods into three types, i.e. **MIA I**, **MIA II** and **MIA III**, based on whether the attacks utilize temporal information and spatial information. **MIA I** corresponds to the method that only uses single temporal information and single spatial information, including the following attacks: black-box attack [Yeom *et al.*, 2018] (referred to as Loss-I), grad-norm attack [Nasr *et al.*, 2019] (Grad-Norm), gradient-diff attack [Li *et al.*, 2022], and Cos attack using single round and single client information (Cos-I). **MIA II** corresponds to the method that uses multiple temporal information and single spatial information, including the following attacks: fed-loss attack [Li *et al.*, 2022] (Loss-II) and Cos attack based on multi-round synchronization (Loss-II). **MIA III** corresponds to the method that uses multiple temporal information and multiple spatial information, including Loss-III and Cos-III.

Evaluation metric. We use metric AUC and TPR@FPR Carlini *et al.* [2022] metric to specifically assess the leakage of the most vulnerable samples to attacks, where TPR@FPR refers to the True Positive Rate (TPR) at a specific False Positive Rate (FPR a.k.a. Type-I Error Rate) in binary classification. Specifically, we pay particular attention to the TPR when the FPR is very low, such as FPR values of 1% or 0.1%. Moreover, we leverage the test error rate as the utility loss, where the smaller test error rate represents achieving the better utility.

4.2 Performance of attack methods

The results of all attacks are presented in the Tab. 2. Based on the existing classification, we can observe that attacks using only Single Temporal Information and Single Spatial Information, specifically MIA I have poor performance, with results on some datasets close to random guessing. For example, the TPR@FPR of Loss-I on CIFAR100 is only 0.3%, rendering it completely ineffective. However, when we incorporate Multiple Temporal Information, specifically MIA II, the attack’s effectiveness improves significantly, especially in terms of the TPR@FPR metric. For instance, the TPR@FPR of the Loss-II attack increases to 14.43%. Finally, when we consider Multiple Temporal Information with MIA III, the attack achieves the strongest performance. For instance, the TPR@FPR of the Loss-III attack increases to 28.79%. Thus, we can conclude that leveraging Temporal and Spatial Information can significantly enhance attack effectiveness.

In terms of MDM selection, we find that cosine similarity outperforms the loss function in the majority of scenarios. The reason is that the gradients of large over-parameterized neural network models statistically behave like high-dimensional independent isotropic random vectors. Therefore, even after multiple local updates, the gradient of training samples can be detected by using cosine similarity. Li *et al.* [2022].

Table 2: Comparison of different MIAs methods on CIFAR100 and Dermnet.

	MIA methods	CIFAR100 AlexNet		CIFAR100 ResNet18		Dermnet AlexNet		Dermnet ResNet18	
		TPR@FPR=1%	AUC	TPR@FPR=1%	AUC	TPR@FPR=1%	AUC	TPR@FPR=1%	AUC
MIA I	Loss-I Yeom <i>et al.</i> [2018]	0.30±0.42	0.62±0.03	1.04±0.11	0.57±0.05	0.43±0.13	0.69±0.05	0.53±0.75	0.53±0.02
	Grad-Diff Li <i>et al.</i> [2022]	1.09±0.23	0.51±0.01	1.04±0.17	0.51±0.01	1.20±0.63	0.52±0.08	1.22±0.26	0.50±0.01
	Grad-Norm Nasr <i>et al.</i> [2019]	1.16±0.11	0.50±0.01	1.13±0.21	0.50±0.01	0.87±0.24	0.49±0.01	1.00±0.23	0.49±0.01
MIA II	Cos-I Li <i>et al.</i> [2022]	8.24±2.37	0.67±0.03	8.54±1.44	0.72±0.01	6.41±4.07	0.74±0.06	6.26±2.93	0.65±0.01
	Loss-II Li <i>et al.</i> [2022]	14.43±2.19	0.69 ± 0.01	8.06±0.25	0.63±0.01	11.47±10.66	0.73 ± 0.01	11.47±10.56	0.57 ± 0.01
	Cos-II Li <i>et al.</i> [2022]	7.24±0.82	0.79 ± 0.01	8.69±0.98	0.80 ± 0.02	12.00±11.60	0.82 ± 0.03	8.20±4.06	0.70 ± 0.01
MIA III	Loss-III (Ours)	28.79±2.45	0.83±0.01	25.60±2.15	0.82±0.00	16.03±13.72	0.87±0.01	17.40±16.87	0.74±0.01
	Cos-III (Ours)	34.00±0.45	0.84±0.02	32.51±2.47	0.84±0.00	15.57±12.78	0.86±0.01	20.00 ± 1.60	0.77 ± 0.02

4.3 Influence of Factors in FL on MIAs

In order to analyze the relationship between FL membership leakage and certain FL setting factors, we conducted additional experiments with different Non-IID extent, communication rounds, numbers of clients, numbers of samples, and local epochs. We use Cos-III attack for all experiments as we have shown that it demonstrates good attack performance in all scenarios. This subsection uses TPR@FPR=1% as the indicator to evaluate the MIA effect. The results and analysis using the Area Under Curve (AUC) value as the indicator can be found in Appendix B.

Non-IID extent. We investigate the impact of non-IID on MIA attacks. Following Hsu *et al.* [2019], the basic assumption of non-iid simulation in this part is that the labels of each client’s training data follow the Dirichlet distribution. β is the core parameter controlling the distribution difference and the smaller the β , the greater the degree of non-iid. We report the performance of the Cos-III attack on the CIFAR-100 dataset in a table. We control the degree of non-IID by adjusting the parameter alpha, where a smaller alpha indicates a more severe non-IID condition. Based on the results, we can observe the following:

As non-IID increases, both attack metrics AUC and TPR show a decreasing-then-increasing trend. There are two reasons for this. First, as non-IID increases, the effectiveness of using other clients as shadow models declines, leading to a decrease in attack performance. Second, when non-IID becomes severe, such as when a client contains only a few classes, MIA attacks themselves become easier. An extreme example is when a client contains only one class, in which case we can achieve a strong baseline by simply judging based on the sample labels.

Communication round. As for the benefits of synchronous rounds to our scheme, it can be observed in Figure 2 (a) and (e) that the attack effect of our scheme increases rapidly in

Table 3: The impact of Non-IID extent on COS-III attacks. The dataset is CIFAR-100.

	AlexNet	AlexNet	ResNet	ResNet
	TPR@FPR=1%	AUC	TPR@FPR=1%	AUC
IID	34.00	0.84	32.51	0.84
$\beta = 100$	10.86	0.82	10.25	0.82
$\beta = 5$	8.98	0.82	8.59	0.80
$\beta = 0.5$	8.66	0.88	7.43	0.87
$\beta = 0.1$	11.22	0.93	10.80	0.93

most epochs as the synchronous communication progresses. At epoch=200, the TPR@FPR=1% of Ours exceeds 0.4, which is twice as high as that of the cosine attack and fed loss attack. After that, the attack effect shows a slight decrease (about 5% on TPR@FPR=1%) and a similar trend can also be observed in the curve of the cosine attack. This phenomenon may be attributed to the fact that the information obtained in the later epochs is not as helpful for the membership leakage attack as the information acquired in the previous epochs.

Number of Clients. Figure 2(b) and (f) illustrate the effects of membership inference attacks on AlexNet and ResNet18, while varying the number of clients from 2 to 20. As depicted in the figures, our two attacks outperform the baselines in most cases, indicating their significantly higher effectiveness. Furthermore, the gradually rising red and blue curves indicate that as the number of clients increases, the target model becomes more vulnerable to our MIA scheme.

Number of Samples. Figure 2(c) and (g) demonstrate the impact of varying the number of samples (ranging from 500 to 5000) on the attack effects of MIAs on AlexNet and ResNet18. Regardless of the increase in the number of samples, the attack effect of our scheme remains consistently high and even demonstrates notable improvement on AlexNet. The

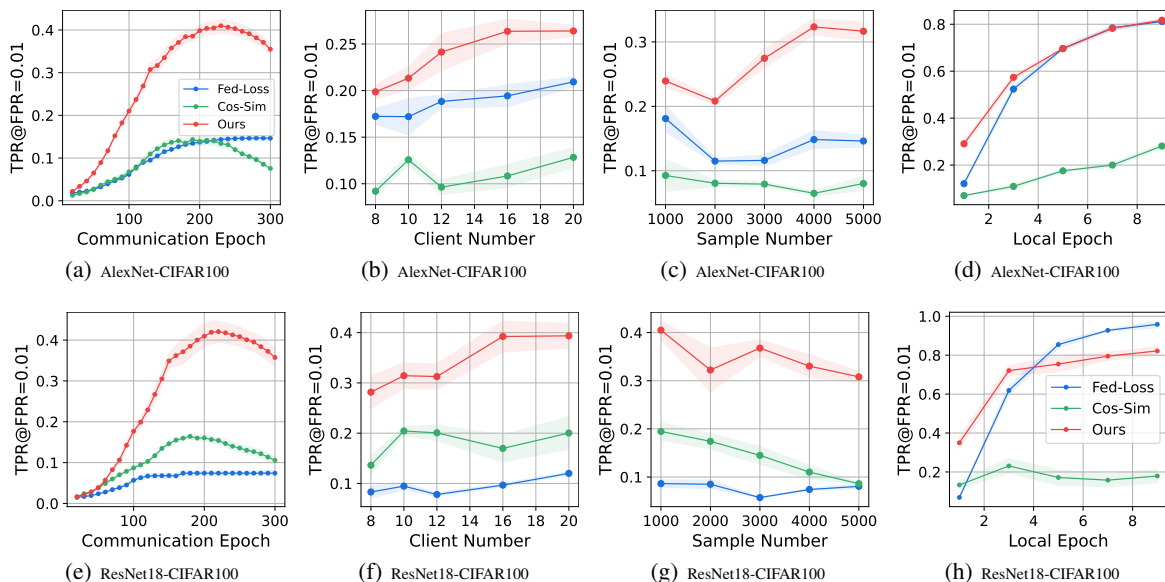


Figure 2: This set of figures shows the attack effects (TPR@FPR=1%) of various attacks (blue line: Loss-II Li *et al.* [2022], green line: Cos-II Li *et al.* [2022] and red line: Cos-III) on AlexNet and ResNet18 (the first and second row respectively) under four settings. The four columns of the graph group show the results of different communication rounds, client numbers, data volumes and local epochs settings respectively.

TPR@FPR=1% of Ours consistently exceeds twice that of the baseline in both subfigures. This indicates that our attack scheme maintains a significant advantage as the training data increases.

Local Epoch. Figure 2(d) and (h) illustrate the effects of MIAs on AlexNet and ResNet18 as the number of local epochs varies from 1 to 9. As the number of local epochs increases, the effectiveness of our attack method and the fed loss attack significantly improve while the enhancement effect of the cosine attack is not evident. This demonstrates that an increase in the number of local epochs may render the model more susceptible to MIA.

5 Defenses Against the Membership Attacks

Several defense ideas have been proposed to mitigate the risks of membership inference. We categorize defenses methods into two clusters: one is to implement protection on the uploaded gradients, called **Gradient Perturbation** method; the other is to implement protection on the training data directly, called **Data Replacement** method.

5.1 Gradient Perturbation

Client-level Differential Privacy. Differential Privacy (DP) Geyer *et al.* [2017]; Zheng *et al.* [2021] hides the membership of individual data by clipping the gradients at the client level and adding Gaussian noise. The magnitude of the noise controls the strength of privacy protection: the larger the noise, the better the privacy protection, but the worse the model’s performance.

Gradient Quantization. Gradient quantization Reisizadeh *et al.* [2020]; Haddadpour *et al.* [2021] is a technique used

to reduce the precision of gradient updates and mitigate information leakage. This algorithm quantizes the values of gradients into discrete approximations, reducing the precision of the gradients. By reducing the detailed information in the gradients, it lowers the sensitivity to individual data and improves privacy protection. The number of bits used for quantization affects the privacy protection effectiveness, where fewer bits introduce larger gradient errors but provide better privacy protection.

Gradient Sparsification. The gradient sparsification algorithm Gupta and Raskar [2018]; Shokri and Shmatikov [2015]; Thapa *et al.* [2022] reduces the risk of information leakage by setting smaller absolute value elements in the gradient to zero. The fewer non-zero elements in the gradient, the less privacy leakage occurs.

5.2 Data Replacement

MixUp. MixUp data augmentation Zhang *et al.* [2017] trains neural networks on composite images created via linear combination of image pairs. It has been shown to improve the generalization of the neural network and stabilizes the training. Based on MixUp, InstaHide was proposed by Huang *et al.* [2020] could protect privacy better with sacrificing the model performance Gu *et al.* [2023].

6 Evaluation of Attacks and Defenses.

6.1 Experimental Setup

In order to facilitate a unified comparison of the aforementioned defense algorithms, we selected the CIFAR-100 dataset and utilized AlexNet and ResNet-18 as the backbone networks. We implemented and executed the aforementioned defense

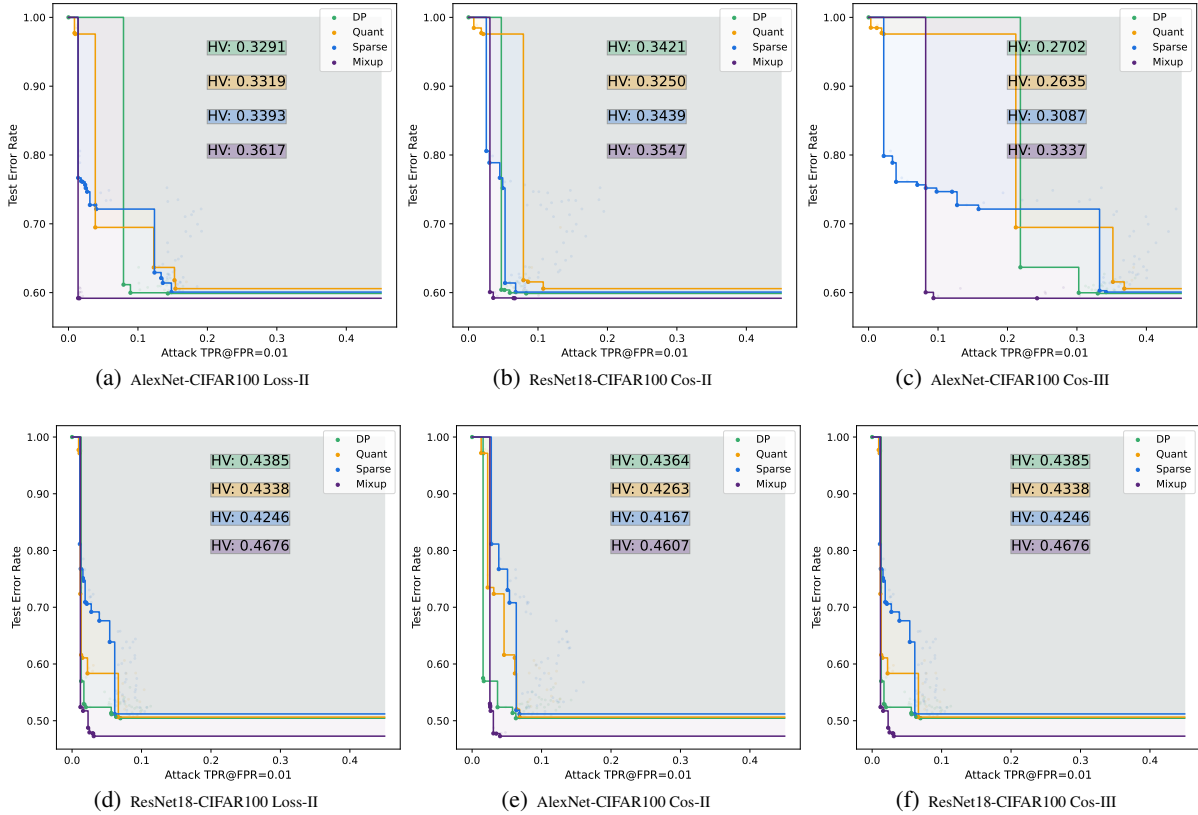


Figure 3: Figure (a)-(f) demonstrate the TPR@FPR=0.01 of various defence (including client-level differential privacy (green line) Geyer *et al.* [2017], gradient quantization (yellow line) Reiszadeh *et al.* [2020], and gradient sparsification (blue line) Shokri and Shmatikov [2015]) under three attacks (Loss-II, Cos-II Li *et al.* [2022] and Cos-III Li *et al.* [2022] are first, second and third row respectively). A larger hypervolume (HV) Zitzler and Künzli [2004] indicates a better Pareto front of privacy and utility.

methods by adjusting the parameters of each method to control the strength of protection. For Differential Privacy, we adjusted the standard deviation of the added Gaussian noise. For Gradient Quantization, we adjusted the bit values after quantization. For Gradient Sparsification, we adjusted the sparsity ratio. For Mixup, we adjusted the random distribution of the mixing coefficient.

Simultaneously, we considered three attack methods: Loss-II, Cos-II, and Cos-III. We adopted TPR@FPR=1% as the evaluation metric for the attacks, and classification accuracy as the utility metric. Due to the inherent trade-off between privacy and utility, the effectiveness of a defense solution can be measured using hypervolume(HV) Zitzler and Künzli [2004], which, in our case, refers to the area between the Pareto frontiers and the unit box. A larger hypervolume indicates a better privacy-utility trade-off.

6.2 Performance of defense methods

Figure 3 presents the Pareto front of privacy and utility. From the Figure 3, we can draw the following conclusions: 1) Our method exhibits the strongest attack. For the same defense method, the hypervolume obtained under the other two attacks is larger than the value calculated under our attack. 2) In the majority of settings, mixup dominates over the other methods,

and in all cases, Mixup achieves the largest hypervolume (HV). This indicates that using mixup as a defense against MIA attacks is a promising choice. 3) In certain scenarios, an excessively strong defense can lead to model training failure, as shown in Figure 3(c).

7 Conclusion

The main objective of this paper is to comprehensively evaluate Membership Inference Attacks and their defenses in the context of federated learning. This paper initially discovers the trend of MIAs in FL. Specifically, incorporating Multi-temporal and Multi-spatial model information enhance the effectiveness of MIAs in FL.

We employ the improved attack strategy to test various federated learning settings and existing defense methods. However, we find that the existing methods such as gradient perturbation methods fail to achieve a satisfactory privacy-utility trade-off while data replacement methods can have a better generalization to resist MIAs.

In summary, we aim to assist researchers in gaining a better understanding of privacy leakage in federated learning and to introduce the more strong defense methods against MIA.

References

- Amina Aboulmira, Hamid Hrimech, and Mohamed Lachgar. Comparative study of multiple cnn models for classification of 23 skin diseases. *International Journal of Online & Biomedical Engineering*, 18(11), 2022.
- Nicholas Carlini, Steve Chien, Milad Nasr, Shuang Song, Andreas Terzis, and Florian Tramer. Membership inference attacks from first principles. In *2022 IEEE Symposium on Security and Privacy (SP)*, pages 1897–1914. IEEE, 2022.
- Jiale Chen, Jiale Zhang, Yanchao Zhao, Hao Han, Kun Zhu, and Bing Chen. Beyond model-level membership privacy leakage: an adversarial approach in federated learning. In *2020 29th International Conference on Computer Communications and Networks (ICCCN)*, pages 1–9. IEEE, 2020.
- Christopher A Choquette Choo, Florian Tramer, Nicholas Carlini, and Nicolas Papernot. Label-only membership inference attacks. *arXiv preprint arXiv:2007.14321*, 2020.
- Jonas Geiping, Hartmut Bauermeister, Hannah Dröge, and Michael Moeller. Inverting gradients-how easy is it to break privacy in federated learning? *Advances in Neural Information Processing Systems*, 33:16937–16947, 2020.
- Robin C Geyer, Tassilo Klein, and Moin Nabi. Differentially private federated learning: A client level perspective. *arXiv preprint arXiv:1712.07557*, 2017.
- Yuhao Gu, Yuebin Bai, and Shubin Xu. Cs-mia: Membership inference attack based on prediction confidence series in federated learning. *Journal of Information Security and Applications*, 67:103201, 2022.
- Hanlin Gu, Jiahuan Luo, Yan Kang, Lixin Fan, and Qiang Yang. Fedpass: Privacy-preserving vertical federated deep learning with adaptive obfuscation. *arXiv e-prints*, pages arXiv–2301, 2023.
- Otkrist Gupta and Ramesh Raskar. Distributed learning of deep neural network over multiple agents. *Journal of Network and Computer Applications*, 116:1–8, 2018.
- Farzin Haddadpour, Mohammad Mahdi Kamani, Aryan Mokhtari, and Mehrdad Mahdavi. Federated learning with compression: Unified analysis and sharp guarantees. In *International Conference on Artificial Intelligence and Statistics*, pages 2350–2358. PMLR, 2021.
- Tzu-Ming Harry Hsu, Hang Qi, and Matthew Brown. Measuring the effects of non-identical data distribution for federated visual classification. *arXiv preprint arXiv:1909.06335*, 2019.
- Yangsibo Huang, Zhao Song, Kai Li, and Sanjeev Arora. Instahide: Instance-hiding schemes for private distributed learning. In *International conference on machine learning*, pages 4507–4518. PMLR, 2020.
- Bo Hui, Yuchen Yang, Haolin Yuan, Philippe Burlina, Neil Zhenqiang Gong, and Yinzhi Cao. Practical blind membership inference attack via differential comparisons. *arXiv preprint arXiv:2101.01341*, 2021.
- Yan Kang, Hanlin Gu, Xingxing Tang, Yuanqin He, Yuzhu Zhang, Jinnan He, Yuxing Han, Lixin Fan, and Qiang Yang. Optimizing privacy, utility and efficiency in constrained multi-objective federated learning. *arXiv preprint arXiv:2305.00312*, 2023.
- Jakub Konečný, H Brendan McMahan, Daniel Ramage, and Peter Richtárik. Federated optimization: Distributed machine learning for on-device intelligence. *arXiv preprint arXiv:1610.02527*, 2016.
- Alex Krizhevsky, Vinod Nair, and Geoffrey Hinton. Cifar-10 (canadian institute for advanced research).
- Hongkyu Lee, Jeehyeong Kim, Seyoung Ahn, Rasheed Husain, Sunghyun Cho, and Junggab Son. Digestive neural networks: A novel defense strategy against inference attacks in federated learning. *computers & security*, 109:102378, 2021.
- Jiacheng Li, Ninghui Li, and Bruno Ribeiro. Effective passive membership inference attacks in federated learning against overparameterized models. In *The Eleventh International Conference on Learning Representations*, 2022.
- Jiacheng Li, Ninghui Li, and Bruno Ribeiro. Effective passive membership inference attacks in federated learning against overparameterized models. In *The Eleventh International Conference on Learning Representations*, 2023.
- H Brendan McMahan, Eider Moore, Daniel Ramage, and Blaise Agüera y Arcas. Federated learning of deep networks using model averaging. *arXiv preprint arXiv:1602.05629*, 2016.
- Brendan McMahan, Eider Moore, Daniel Ramage, Seth Hampson, and Blaise Agüera y Arcas. Communication-efficient learning of deep networks from decentralized data. In *Proceedings of Artificial Intelligence and Statistics (AISTATS)*, pages 1273–1282, 2017.
- Milad Nasr, Reza Shokri, and Amir Houmansadr. Comprehensive privacy analysis of deep learning: Passive and active white-box inference attacks against centralized and federated learning. In *2019 IEEE symposium on security and privacy (SP)*, pages 739–753. IEEE, 2019.
- Amirhossein Reisizadeh, Aryan Mokhtari, Hamed Hassani, Ali Jadbabaie, and Ramtin Pedarsani. Fedpaq: A communication-efficient federated learning method with periodic averaging and quantization. In *International Conference on Artificial Intelligence and Statistics*, pages 2021–2031. PMLR, 2020.
- Shahbaz Rezaei and Xin Liu. Towards the infeasibility of membership inference on deep models. *arXiv preprint arXiv:2005.13702*, 2020.
- Alexandre Sablayrolles, Matthijs Douze, Yann Ollivier, Cordelia Schmid, and Hervé Jégou. White-box vs black-box: Bayes optimal strategies for membership inference. In *International Conference on Machine Learning (ICML)*. PMLR, 2019.
- Ahmed Salem, Yang Zhang, Mathias Humbert, Mario Fritz, and Michael Backes. MI-leaks: Model and data independent membership inference attacks and defenses on machine learning models. In *Annual Network and Distributed System Security Symposium (NDSS)*, 2019.

- Reza Shokri and Vitaly Shmatikov. Privacy-preserving deep learning. In *Proceedings of the 22nd ACM SIGSAC conference on computer and communications security*, pages 1310–1321, 2015.
- Reza Shokri, Marco Stronati, Congzheng Song, and Vitaly Shmatikov. Membership inference attacks against machine learning models. In *2017 IEEE symposium on security and privacy (SP)*, pages 3–18. IEEE, 2017.
- Liwei Song and Prateek Mittal. Systematic evaluation of privacy risks of machine learning models. *arXiv preprint arXiv:2003.10595*, 2020.
- Chandra Thapa, Pathum Chamikara Mahawaga Arachchige, Seyit Camtepe, and Lichao Sun. Splitfed: When federated learning meets split learning. In *Proceedings of the AAAI Conference on Artificial Intelligence*, volume 36, pages 8485–8493, 2022.
- Larry E Toothaker. *Multiple comparison procedures*. Number 89. Sage, 1993.
- Stacey Truex, Ling Liu, Mehmet Emre Gursoy, Lei Yu, and Wenqi Wei. Demystifying membership inference attacks in machine learning as a service. *IEEE Transactions on Services Computing*, 2019.
- Yuanyuan Xie, Bing Chen, Jiale Zhang, and Di Wu. Defending against membership inference attacks in federated learning via adversarial example. In *2021 17th International Conference on Mobility, Sensing and Networking (MSN)*, pages 153–160. IEEE, 2021.
- Qiang Yang, Yang Liu, Tianjian Chen, and Yongxin Tong. Federated machine learning: Concept and applications. *ACM Transactions on Intelligent Systems and Technology (TIST)*, 10(2):1–19, 2019.
- Samuel Yeom, Irene Giacomelli, Matt Fredrikson, and Somesh Jha. Privacy risk in machine learning: Analyzing the connection to overfitting. In *2018 IEEE 31st computer security foundations symposium (CSF)*, pages 268–282. IEEE, 2018.
- Oualid Zari, Chuan Xu, and Giovanni Neglia. Efficient passive membership inference attack in federated learning. *arXiv preprint arXiv:2111.00430*, 2021.
- Hongyi Zhang, Moustapha Cisse, Yann N Dauphin, and David Lopez-Paz. mixup: Beyond empirical risk minimization. *arXiv preprint arXiv:1710.09412*, 2017.
- Jingwen Zhang, Jiale Zhang, Junjun Chen, and Shui Yu. Gan enhanced membership inference: A passive local attack in federated learning. In *ICC 2020-2020 IEEE International Conference on Communications (ICC)*, pages 1–6. IEEE, 2020.
- Qinqing Zheng, Shuxiao Chen, Qi Long, and Weijie Su. Federated f-differential privacy. In *International Conference on Artificial Intelligence and Statistics*, pages 2251–2259. PMLR, 2021.
- Ligeng Zhu, Zhijian Liu, and Song Han. Deep leakage from gradients. *Advances in neural information processing systems*, 32, 2019.
- Eckart Zitzler and Simon Künzli. Indicator-based selection in multiobjective search. In *International conference on parallel problem solving from nature*, pages 832–842. Springer, 2004.

A Experiment details and additional results

A.1 Dataset and Training Details

The CIFAR-100 dataset consists of 100 categories with 60,000 32×32 color images, where 50,000 images are allocated for training and 10,000 images for testing. The Dermnet dataset includes 23 categories with a total of 19,500 images, where 15,500 images are allocated for training and 4,000 images for testing. Since the images have varying sizes, we cropped them to a size of 64×64 pixels. The training parameters details of federated learning are shown in Table 4.

A.2 Evaluation Metrics

Utility loss (Test error rate). In this paper, we quantify the utility loss by using the test error as a metric. The test error measures the accuracy of the model on a separate test dataset, where a lower test error indicates better model utility. The worst possible test error rate is 1, which means that the model makes incorrect predictions for all instances in the test dataset.

Privacy Leakage (AUC and attack TPR) We consider attacks as a binary classification task, and the TPR@FPR of the AUC can be used to measure the accuracy of the classification, which represents the effectiveness of the attack. TPR@low FPR is a metric recently proposed for measuring MIA (Membership Inference Attack). It focuses more on the data that is most susceptible to attacks, and researchers believe that using it as a metric can better characterize privacy protection in worst-case scenarios.

TPR (True Positive Rate) and FPR (False Positive Rate) are two important metrics used to evaluate the performance of binary classification models, such as machine learning algorithms or diagnostic tests. They are calculated as follows:

$$\text{TPR} = \text{TP} / (\text{TP} + \text{FN})$$

$$\text{FPR} = \text{FP} / (\text{FP} + \text{TN})$$

where: TP (True Positives) represents the number of positive instances correctly classified as positive. FN (False Negatives) represents the number of positive instances incorrectly classified as negative. FP (False Positives) represents the number of negative instances incorrectly classified as positive. TN (True Negatives) represents the number of negative instances correctly classified as negative.

Hypervolume $HV(\cdot)$. In order to compare Pareto fronts achieved by different defense algorithms, we need to quantify the quality of a Pareto front. To this end, we adopt the hypervolume (HV) indicator Zitzler and Künzli [2004] as the metric to evaluate Pareto fronts. Definition 1 formally defines the hypervolume.

Definition 1 (Hypervolume Indicator). *Let $z = \{z_1, \dots, z_m\}$ be a reference point that is an upper bound of the objectives $Y = \{y_1, \dots, y_m\}$, such that $y_i \leq z_i, \forall i \in [m]$. the hypervolume indicator $HV_z(Y)$ measures the region between Y and z and is formulated as:*

$$HV_z(Y) = \Lambda \left(\left\{ q \in \mathbb{R}^m \mid q \in \prod_{i=1}^m [y_i, z_i] \right\} \right) \quad (13)$$

where $\Lambda(\cdot)$ refers to the Lebesgue measure.

We set the reference point z of privacy leakage and utility loss to be 1 and 100% respectively.

B AUC Results of Ablation Study

In this section, we show the experimental results using the Area Under Curve (AUC) value of Receiver Operating Characteristic (ROC) as an indicator to evaluate the attack effect of ablation study.

Communication Epoch. Similar to the results of Sect 4, as the communication epoch increases, the effect of our proposed attack scheme is always better than baselines. The AUC curve increases rapidly in the first 150 epochs, reaches a maximum around 200 epochs, and then declines slightly, which is consistent with the performance of TPR.

Number of Clients. As the number of clients increases, the MIA attack effect tends to increase, which is similar to TPR results. Besides, the AUC curve of our scheme is always higher than other baseline schemes and the value is always over 0.80.

Number of Samples. When the number of samples in the training set of each client changes from 1000 to 5000, the AUC value of our scheme is always higher than the baselines, maintaining above 0.80 on both models.

Local Epoch. With the increase of local epoch, the AUC of the three MIA schemes all increase significantly, among which the fed-loss attack has the largest increase rate. But in most cases, our scheme is higher than the two baselines.

Table 4: Training parameters for federated learning in this paper

Dataset	CIFAR100	Dermnet
Models	AlexNet, ResNet18	AlexNet, ResNet18
Communication epoch	300	300
Optimizer	SGD	SGD
Initial learning rate	0.1	0.1
Learning rate decay	0.99 at each communication epoch	0.99 at each communication epoch
Number of clients	10	10
Training set size for one client	5000	1500
Testing set size	10000	4500

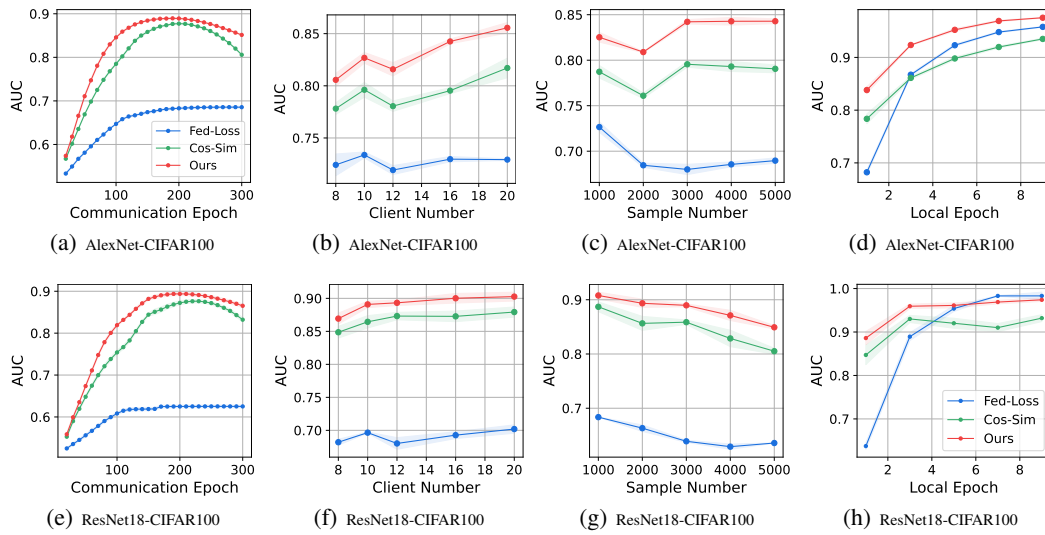


Figure 4: This set of figures shows the attack effects (AUC) of various attacks on AlexNet and ResNet18 (the first and second row respectively) under four settings. The four columns of the graph group show the results of different communication rounds, client numbers, data volumes and local epochs settings respectively.